Fuel 262 (2020) 116493

Contents lists available at ScienceDirect

Fuel

journal homepage: www.elsevier.com/locate/fuel

Full Length Article

Effect of the temperature on the spent coffee grounds torrefaction process in a continuous pilot-scale reactor

M. Barbanera[a,b,*], I.F. Muguerza[c]

[a] Department of Economics, Engineering, Society and Business Organization, University of Tuscia, 01100 Viterbo, Italy
[b] Biomass Research Centre University of Perugia, Via G. Duranti 67, 06125 Perugia, Italy
[c] National Renewable Energy Centre (CENER), C/Ciudad de la Innovación 7, 31621 Sarriguren, Navarra, Spain

ARTICLE INFO

Keywords:
Torrefaction
Spent coffee grounds
Mass yield
Energy yield
Product properties

ABSTRACT

Several studies in Literature have analyzed the torrefaction treatment process of biomass in batch reactors. Nevertheless, in order to check the industrial applicability of a process, it is more interesting to carry out torrefaction tests in continuous pilot plant reactors. Thus, the present study reports the results of continuous semi-industrial scale (500 kg/h) torrefaction experiments employing spent coffee grounds (SCG) as a feedstock in a horizontal rotary reactor. Torrefaction tests were carried out at three different temperatures (210 °C, 235 °C, and 260 °C) for 90 min, in order to evaluate the yields of solid, liquid (water and tar) and gaseous products and their composition. In particular, the effectiveness of the decarbonization and deoxygenation processes was investigated, analyzing the carbon and oxygen distribution. Within the temperature range, torrefaction yielded solid of 55.2–85.8 wt% with an increase of the higher heating value (HHV) of 5.1–15.4% compared to the raw material. Liquid fraction yield was in the range of 11.3–34.3 wt%, with a moisture content of 73.7–91.9% and HHV between 18.8 and 23.4 MJ/kg on dry basis. Gas fraction represented 2.9–10.5 wt% of the raw biomass with HHV between 1.95 and 3.55 MJ/Nm^3. Acids (mainly acetic acid) were the major compounds in the tar fraction, accounted up to 68 wt%, while CO_2 was the main product of the deoxygenation reactions in the gaseous fraction (76.6–86.9 vol%). From the perspective of mass yield and energy density enhancement, 260 °C was considered to be the optimal temperature for torrefaction of SCG.

1. Introduction

Decarbonisation and the promotion of renewable energy sources have become common goals of climate change mitigation around the world. The EU environmental policy has focused mainly on renewable fuels with the aim to diversify energy sources and hit the requirement of energy security. In particular, bioenergy is the most important source of renewable energy in the EU, accounting for about 63.3% of all renewable energy production [1]. However, despite the increase in biomass for energy exploitation, some drawbacks still limit its efficient use because solid biomass is characterized by highly variable composition and chemical-physical properties [2]. In particular, the presence of moisture and the heterogeneity of the organic and inorganic fractions cause technical issues in biomass exploitation for energy production, especially in energy conversion systems based on the combustion process.

Spent coffee grounds (SCG) are one of those solid biomass resources. Coffee is the second largest traded commodity of the world and responsible for a lot of waste [3]. A big share of this waste is SCG (6 millions of tons per year), a product high in lignin and cellulose that is mainly incinerated, disposed in landfill, or composted [4]. However, in the last years there has been a significant increase of the attention given to the bioenergy production from SCG [5].

To date, several pretreatment approaches have been investigated in order to produce biofuels with more homogeneous properties. The most common pretreatments are based on thermochemical processes (gasification, pyrolysis, carbonization, torrefaction), where the biomass is exposed to high temperatures in absence of oxygen or with a low concentration of oxygen [6]. The heat causes the breakdown of the chemical bonds of the organic molecules (cellulose, hemicellulose and lignin) changing the structure or causing the formation of volatile compounds. In particular, the thermal stability of hemicellulose, cellulose, and lignin decreases in this order due to the losses of the carboxyl group from hemicellulose, the carbonyl and the carboxyl groups from cellulose and the aromatic ring and the methoxyl groups from lignin [7].

* Corresponding author at: Department of Economics, Engineering, Society and Business Organization, University of Tuscia, 01100 Viterbo, Italy.
E-mail address: m.barbanera@unitus.it (M. Barbanera).

https://doi.org/10.1016/j.fuel.2019.116493
Received 22 June 2019; Received in revised form 18 October 2019; Accepted 23 October 2019
Available online 08 November 2019
0016-2361/

Among the thermochemical processes, torrefaction has attracted increasing interest among the scientific community both for its energy efficiency and its effectiveness to improve the performance of biomass based fuels. Torrefaction is a thermal pretreatment for solid biomass carried out under an inert atmosphere, at atmospheric pressure and at temperatures of 200–300 °C for several minutes or hours. During the torrefaction process, biomass undergoes several thermochemical reactions, causing the release and thermal decomposition of volatiles and a loss of solid matter that can reach values of even 30% by weight. At the same time, the loss of this fraction determines also an energy loss of about 10–15% of the total energy contained in the raw material [8]. The lower energy loss than the mass loss is mainly due to the breakage of the hydroxyl groups that are replaced by unsaturated non-polar groups, reducing the water adsorbing capacity (hygroscopicity) of the torrefied material which becomes less sensitive to biological degradation [9]. These transformations allow also to reduce the mechanical strength of biomass, obtaining a fuel with increased friability for easier grinding. The solid fraction does not represent the only product of the torrefaction process as it also generates small amounts of liquid and gaseous streams which are still under-exploited [10]. The condensable fraction is a multicomponent mixture, formed by oxygenated species (acids, alcohols, furans, ketones, tarpenes, phenols, tannins) diluted in water, while the non-condensable fraction, also called torgas, is a mixture of gases like CO_2, CO, CH_4, C_xH_y, toluene, and benzene [11]. In particular, the condensable fraction could be exploited for the extraction of several compounds that have interesting applications in the chemical industry [12] or for methane production through anaerobic digestion [13]. Lê Thành et al. [14] detected > 100 condensable species during the torrefaction of pine, ash wood, miscanthus and wheat straw. As regards the non-condensable fraction, its energy content is low (less than 10% of the energy in biomass) but it could be burned with a fraction of raw material in order to satisfy the heat demand of the torrefaction plant improving the overall process efficiency [15]. However, the review of recent literature suggests that scarce attention has been paid to the analysis of gas and liquid products which should be instead considered for improving the economic feasibility of the process [16]. The yields of the products and their composition during the torrefaction process depends on the operating conditions, such as temperature, residence time, heating rate, particle size and reactor type. Among these parameters, temperature is the most important single variable affecting the torrefaction process [17] while residence time has less influence, even if there is a maximum value above which there are no significant differences in terms of torrefaction product properties for each kind of biomass [14]. On the other hand, residence time has a strong influence on the reactor design [18].

In recent years, several studies have evaluated the torrefaction performance by using different types of reactors, such as rotary drum [19,20], moving bed [21], screw conveyor [22], fluidized bed [23], and fixed bed [24]. For example, in the rotary drum torrefier, the rotational speed, the length and the tilt of the drum are determined by the required residence time. However, Chen et al. [25] in their review remarks that most studies have been carried out in lab-scale reactors while it could be useful to examine the scale up effects on the mass and energy balance of the torrefaction process in pilot and demonstration plants.

Until now, torrefaction process of spent coffee grounds was performed only in a thermogravimetric device [26,27] or in a quartz tube reactor [17], focusing the attention on the solid product. In this study, a rotary drum pilot reactor (500 kg/h) was employed in order to evaluate the effect of torrefaction temperature on the properties of solid, liquid and gas products of spent coffee grounds. It is expected that the results obtained in this study will allow to deepen the knowledge about the chemical properties of the torrefaction products for their use for the production of value-added chemicals.

Table 1
Particle size distribution of raw spent coffee grounds.

mm	%
< 0.063	0.0
0.063–0.125	4.8
0.125–0.25	19.2
0.25–0.5	21.2
0.5–0.71	15.7
0.71–1	14.7
1–1.4	18.8
1.4–2	4.5
2–2.5	0.8
2.5–3.15	0.2
> 3.15	0.0

2. Materials and methods

2.1. Feedstock properties

Spent coffee grounds were supplied by by Nestlé Spain (Barcelona). Before starting the torrefaction tests, the raw biomass was dried at 105 °C, for 24 h, in a rotary dryer at the Spanish National Centre of Renewable Energies (CENER) in order to reduce the moisture content from 58% to 10%. Then, the particle size distribution of dried SCG was determined according to the EN ISO 17827-2:2016 (Table 1) by using a vibrating sieve shaker Retsch AS 200 (Retsch Technology, Germany) with nine sieves ranging from 0.063 to 3.15 mm in opening size. Furthermore, the proximate, ultimate, compositional and HHV analysis of dried feedstock were performed and the results are shown in Table 2.

2.2. Torrefaction pilot plant and experimental procedure

The torrefaction pilot plant at the CENER has a nominal production capacity of about 500 kg/h (Fig. 1). The plant is divided into three main sections: the feeding system, the torrefaction reactor and the torrefied product collection section [28].

The feeding system requires that biomass is filled in a hopper with a capacity of 4.2 m^3, and then it is transported through a moving floor conveyor into the torrefaction reactor. The hopper is kept under suction with an integrated bag filter to minimize dust emission. The core of the process is the torrefier based on a horizontal rotary reactor with internal elements designed to attain a homogeneous flow of biomass particles along reactor, and to guarantee excellent heat transfer conditions. The reactor is designed to handle low bulk density biomass (> 50 kg/m^3) with high content of fines and dust. Reactor heating is carried out indirectly through the walls by means of thermal oil as heat transfer fluid. The control system of the torrefaction plant allows to set the inlet temperature of the thermal oil (maximum value is 300 °C) into

Table 2
Characterization of raw and torrefied spent coffee grounds (SCG).

Sample	SCG	SCG-210	SCG-235	SCG-260
Proximate analysis (wt%, dry basis)				
Volatile	82.5 ± 0.2	77.4 ± 0.4	75.6 ± 0.4	70.8 ± 0.2
Ash	0.41 ± 0.05	0.53 ± 0.07	0.58 ± 0.04	0.86 ± 0.11
Fixed Carbon	17.1 ± 0.1	22.1 ± 0.3	23.8 ± 0.3	28.3 ± 0.2
Ultimate analysis (wt%, dry basis)				
C	59.7 ± 0.3	62.2 ± 0.1	63.7 ± 0.2	66.6 ± 0.2
H	7.8 ± 0.5	7.7 ± 0.2	7.7 ± 0.4	7.5 ± 0.1
N	2.2 ± 0.1	2.2 ± 0.1	2.3 ± 0.1	2.7 ± 0.1
S	0.1 ± 0.01	0.1 ± 0.02	0.1 ± 0.01	0.1 ± 0.01
O	30.2 ± 0.7	27.8 ± 0.5	26.2 ± 0.5	23.1 ± 0.4
Higher Heating Value (MJ/kg, dry basis)	25.3 ± 0.5	26.6 ± 0.6	27.3 ± 0.3	29.5 ± 0.7

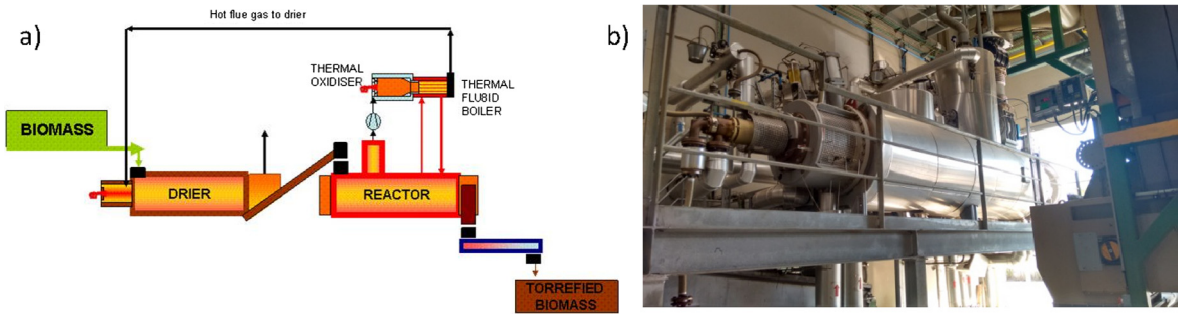

Fig. 1. Scheme of the torrefaction pilot plant and view of the reactor.

the torrefier. Inside the reactor, the temperature is measured by nine type N thermocouples that are uniformly distributed along the rotary kiln. In addition, the temperature of biomass at the end of the reactor is measured and usually it is significantly lower than the reactor temperature set-point, showing that the temperature set-point cannot be assumed as the torrefaction temperature. In this work, the torrefaction of SCG was carried out at three temperature conditions. In particular, the inlet temperature of thermal oil was set at 240, 265, and 290 °C, corresponding to an exit temperature of biomass equal to 210, 235, and 260 °C, respectively. For this reason, the torrefied materials after the tests were named as SCG-210, SCG-235, and SCG-260.

In order to evaluate the energy efficiency of the process, Table 3 shows the average thermal and electrical power required by the pilot-scale reactor during each test and measured by the data acquisition system of the torrefaction plant.

After the torrefaction temperature in the reactor is reached, the torrefier is swept by a continuous nitrogen flow of 9.6 Nm^3/h, in order to maintain the inert atmosphere. Torrefied biomass is removed from the reactor via a water-cooled screw conveyor and it is transported and stored in big-bags. Gas produced during the torrefaction treatment are expelled from the torrefier through a blower and then burned in a thermal oxidiser. The blower speed is set to keep a negative pressure of about 0.5–2 mbar inside the torrefier. The residence time and the feeding rate during torrefaction are regulated by mean of frequency controllers of the rotate speed of the kiln and the moving floor conveyor of the feeding hopper. In our tests, the feeding rate was set at 360 kg/h and the residence time at 90 min. These values were chosen after preliminary tests that highlighted that the reduced size of SCG did not allow to reduce too much the rotational speed of the auger and, thus, the residence time to be less than 90 min. Each torrefaction tests was made to last 1 h after the steady-state conditions were reached that were characterized by steady biomass temperature at the exit of the reactor and steady gas flow rate. During the steady-state conditions, the torrefied material, produced and stored in the big-bags, was weighted in order to calculate the mass yield of the process, permanent gases were determined by continuous on-line sampling and gas conditioning, and the condensate samples were obtained collecting a small fraction (5–10 L/min) of the permanent gases and cooling it in a sampling train.

2.3. Analytical methods

Moisture, ash, and volatile matter content of raw and torrefied biomass were determined in accordance with the technical standards UNI EN ISO 18134–2:2017, UNI EN ISO 18122:2016, and UNI EN ISO 18123:2016, respectively. Proximate analysis was performed by using the thermogravimetric analyzer Leco TGA-701 (LECO Corporation, St. Joseph, MI, USA). Ultimate analysis was carried out according to UNI EN ISO 16948:2015 using the Leco TruSpec CHN analyser (LECO Corporation, St. Joseph, MI, USA). Oxygen content was calculated by difference. The higher heating value (HHV) of solid products was determined with a Leco AC-350 isoperibolic calorimeter (LECO Corporation, St. Joseph, MI, USA) and in accordance to the standard UNI EN ISO 18125:2018. Compositional analysis, in terms of cellulose, hemicellulose, lignin, acetyl groups, and extractives content, was performed in accordance with the analytical methods described in a previous work [29].

For gaseous samples, gas composition concentration was measured according to CENER's internal procedure, according to the IEA Task 33 gas analysis special report [30]. Gas is sampled on-line with a probe and a sampling train for gas conditioning. The outlet of the sampling train is connected to a micro gas chromatograph (Micro-GC 3000A, Agilent Technologies, USA) which measured gas composition each about 3 min. The micro GC was calibrated with certified gas mixture containing H_2, CO, CO_2, N_2, O_2, C_3H_8, C_4H_{10}, C_5H_{12} and C_6H_{14}. The mass fraction of each gas was obtained by multiplying the volume fraction for its density while the calorific value of the gaseous products was calculated by the following equation:

$$\begin{aligned} HHV_{gas}(MJ/Nm^3) = {} & Vol H_2(\%) * HHV_{H2}(MJ/Nm^3) + Vol CO\ (\%) \\ & * HHV_{CO}(MJ/Nm^3) + Vol C_3H_8(\%) * HHV_{C3H8} \\ & (MJ/Nm^3) + Vol C_4H_{10}(\%) * HHV_{C4H10} \\ & (MJ/Nm^3) + Vol C_5H_{12}(\%) * HHV_{C5H12} \\ & (MJ/Nm^3) + Vol C_6H_{14}(\%) * HHV_{C6H14}(MJ/Nm^3) \end{aligned} \quad (1)$$

Condensate products were sampled during gas composition analysis and then analysed by liquid (HPLC-DAD & RID) (HPLC 1100 series, Agilent Technologies, USA) and gas (GC-FID) (7890B, Agilent Technologies, USA) chromatographic techniques. The water content of the liquid sample, corresponding to the gas moisture, was determined by Karl-Fischer titration (V30, Mettler Toledo, OH, USA). Anhydrous magnesium sulfate was added to the remaining liquid fraction in order to separate the organic components of tar from water. Then, ultimate analysis of tar was carried out by Leco TruSpec CHN analyser (LECO Corporation, St. Joseph, MI, USA), calculating the oxygen content by difference. HHV of tar was calculated from its elemental composition (excluding sulfur), according to the Eq. (2) [31]:

$$HHV_{tar}(MJ/kg) = 0.352\ C + 0.944\ H + 0.105(S - O) \quad (2)$$

All the analysis experiments were performed in triplicate, and the average value of data was assumed. Most results were quite uniform between each other. Error bars were omitted but the relative error was mostly less than 5%.

Table 3
Energy requirements of the torrefaction plant.

	SCG-210	SCG-235	SCG-260
Average thermal power (kW)	40.7	46.7	54.5
Average electrical power (kW)	3.0	3.3	3.2

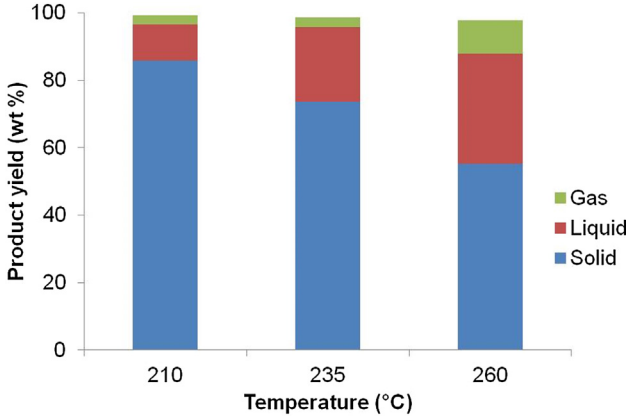

Fig. 2. Distribution of product yields from spent coffee grounds torrefaction.

2.4. Torrefaction process parameters

Mass (Ymass) and energy (EY) yields of torrefied products (solid, liquid, and gaseous), and energy density enhancement of (EDE) torrefied biomass were calculated by using the following equations [32]:

$$Y_{mass} = Mpr/Mraw * 100\% \quad (3)$$

$$EY = Y_{mass} * HHV_{pr}/HHV_{raw} \quad (4)$$

$$EDE = HHV_{pr} - - HHV_{raw}/HHV_{raw} * 100\% \quad (5)$$

where M_{pr} and HHV_{pr} are the mass and higher heating value of solid, liquid, and gaseous products, and M_{raw} and HHV_{raw} represent the mass and higher heating value of raw feedstock.

3. Results

3.1. Mass yields of torrefaction products

Fig. 2 shows the effect of the torrefaction temperature on the yields of solid, liquid, and gas products. The overall mass balance at different temperatures was always above 95.5%, mostly due to the high accuracy in the determination of the solid product which represents the largest fraction of the torrefied products. It is evident that the solid yield decreases while the liquid and gas yields increases when the torrefaction temperature rises from 210 °C to 260 °C. In particular, torrefied SCG was characterized by a mass loss of about 14%, 26% and 45% at 210 °C, 235 °C and 260 °C, respectively, indicating that the torrefaction treatment was more effective between 235 °C and 260 °C. On the other hand, the yields of condensable and non-condensable products increase with temperature from 11% to 34% and from 3% to 11%, respectively, due to the decarboxylation and deoxygenation reactions of the hemicellulose and part of cellulose, causing the formation of water vapour and the release of gases and light volatile organic compounds [33]. It is interesting to note that the torrefaction treatment at 210 °C was quite more significant than that for other kind of biomass. Chen et al. [34] obtained a solid yield of 95.3% at 210 °C for rice husk, while Uemura et al. [35] reported that significant torrefaction did not take place in the oil palm waste samples at a torrefaction temperature of 220 °C. This result could be attributed to the high extractives content (25.2%) in SCG; in fact, the evaporation of extractives begins at 150–220 °C when the breakdown of the most labile bonds occurs with the emission of volatile matter.

3.2. Characterization of solid products

Proximate analysis, ultimate analysis and heating value of the raw SCG and torrefied SCG produced at different temperatures are reported in Table 2.

When the torrefaction temperature increases from 210 °C to 260 °C, the volatile matter decreases from 82.5% to 70.8% at 260 °C as a result of the thermal degradation of SCG. At the same time the fixed carbon and ash content show a significant increase, resulting in enhancement of the fuel ratio (fixed carbon/volatile matter) whose value increases from about 0.2 for raw SCG to 0.4 for torrefied SCG at 260 °C. This result is interesting when biomass is used in cofiring with coal because the lower value of fuel ratio of biomass could cause a non-uniform heat distribution inside the combustion chamber [36].

Ultimate analysis showed that carbon content increased up to 11% when the torrefaction temperature reached 260 °C while hydrogen and oxygen content was decreased with increasing temperature. In particular, the most significant change was registered for the oxygen content when the temperature increased from 235 °C to 260 °C, reaching a decrease of about 23.5% compared to raw SCG. The reduction of oxygen and hydrogen content was mainly due to the decarboxylation and deoxygenation reactions and to the removal of the carboxyl groups, respectively [35]. Moreover, as a result of devolatilization, the calorific value of torrefied biomass significantly raised with the temperature, observing an increase of HHV of about 5% at low-temperature torrefaction and of about 17% at 260 °C (29.5 MJ/kg). This trend of HHV can be associated to the ultimate analysis where an increase in the carbon content leads to increase of calorific value.

Fig. 3 shows the Van Krevelen diagram where the atomic H/C and O/C ratios of SCG before and after torrefaction are plotted, in order to analyze the evolution of the composition of biomass as function of the torrefaction temperature. It can be seen that the H/C and O/C atomic ratios decrease as temperature increase due to drying and devolatilization process [37], approaching to the typical values for coal. Furthermore, the relationship between the elemental compositions of raw and torrefied SCG could be expressed by a linear equation, having a slope of 1.79; this result indicates that the torrefaction treatment was more effective on the H/C ratio than the O/C ratio by a factor of about 1.8. This trend was quite different from that obtained by Zhang et al. [17]; they determined a value of slope of about 1.2 but the torrefaction tests were carried out in a lab-scale tubular furnace and not in a continuous pilot-scale reactor.

Compositional analysis of raw and torrefied SCG was reported in Table 4. It can be noted that hemicellulose is the most reactive polymer because its content was strongly influenced by the torrefaction temperature. Thermal degradation of hemicellulose occurs between 200 and 280 °C with the removal of the carboxyl groups and the release of CO_2, CO, H_2O, and oxygen-containing organic compounds [39].

On the other hand, cellulose was subjected to a partial depolymerization starting at 235 °C because its content in biomass first increased from 16.5% to 17.5% at 210 °C and then, it decreased to 11.7% at 260 °C. This result was in accordance with the typical decomposition

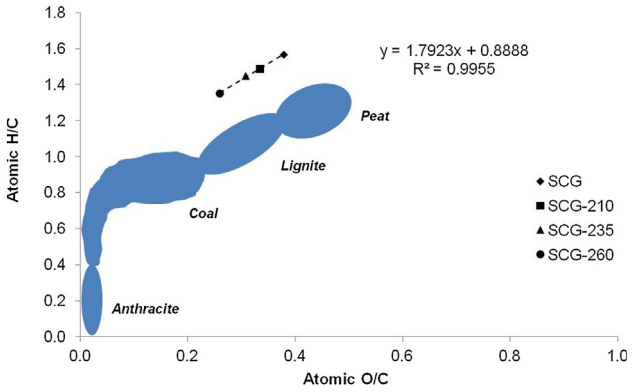

Fig. 3. Van Krevelen diagram of torrefied spent coffee grounds (SCG) at different torrefaction temperatures. Typical values of the atomic ratios for different grades were taken from Van der Stelt et al. [38].

Table 4
Compositional analysis of raw and torrefied SCG.

Component	SCG	SCG-210	SCG-235	SCG-260
Hemicellulose (wt%, dry basis)	22.8 ± 0.3	21.0 ± 0.2	12.4 ± 0.2	3.3 ± 0.1
Cellulose (wt%, dry basis)	16.5 ± 0.5	17.5 ± 0.4	13.8 ± 0.2	11.7 ± 0.1
Acid Insoluble Lignin (wt%, dry basis)	32.7 ± 1.1	33.1 ± 0.9	36.8 ± 0.7	39.5 ± 0.5
Acetyl Groups (wt%, dry basis)	0.21 ± 0.03	0.18 ± 0.02	0.11 ± 0.04	0.13 ± 0.02
Extractives (wt%, dry basis)	25.2 ± 0.5	26.8 ± 0.6	35.7 ± 0.3	42.9 ± 0.4
Other (wt%, dry basis)	2.6 ± 0.2	1.4 ± 0.1	1.2 ± 0.1	2.5 ± 0.2

temperature range for cellulose (240–350 °C) [40]. Lignin is the most thermally stable component of biomass because it decomposes over a wide temperature range (230–550 °C) and its increase could be due both to the decrease in the polysaccharide content and to the partial carbonization of sugars when the torrefaction temperature increases. In fact, the carbonized sugars could not be dissolved during the acid treatment of the compositional analysis procedure, causing an increase of the acid insoluble lignin content. Extractives are the non-structural components of biomass and their content in the torrefied biomass should decrease by devolatilization with the temperature. However, SCG shows an opposite trend that can be explained by the accumulation of by-products, arising from the partial degradation of lignin and holocellulose. These residues were maybe subjected to chemical and physical changes in their structure that made them not-separable from the solvents used in the analyses [41].

3.3. Characterization of permanent gases

The main components of the non-condensable gases were CO and CO_2 with a small amount of H_2, C_3H_8, C_5H_{12}, and C_6H_{14}, depending on the torrefaction temperature. Table 5 shows the non-condensable gases yield and it can be noted that the yield and composition of gases were strongly affected by the operating conditions.

Carbon monoxide and carbon dioxide yields increased as the torrefaction temperature raised, demonstrating that a significant amount of oxygen was removed from biomass and transferred from SCG into permanent gas. Up to the temperature of 235 °C, the overall permanent gas yield was very low (about 3 wt%) while a quick increase occurred at 260 °C (about 10.5%) when the CO_2 concentration was reduced to about 77% (v/v) and the CO fraction in the permanent gas increased to about 22.5% (v/v). These results can be explained by the breakdown of the lignocellulosic components at different temperatures, as discussed previously. In particular, carbon monoxide mainly comes both from decarbonylation reaction of low mass species, obtained during the degradation of hemicellulose, and the reaction between carbon dioxide and steam with char; on the other hand, the formation of CO_2 can be explained by the decarboxylation of some acid groups present in the hemicellulose, such as uronic acid of xylan [39]. Moreover, as the temperature increases, the ratio of carbon monoxide to carbon dioxide tends to increase from 14.7% (v/v) to 29.3% (v/v). These values were in line with those achieved for other kind of biomass, such as willow and larch [42], while they were quite lower compared to the Eupatorium adenophorum Spreng, for which Han et al. [32] obtained a ratio of about 55% (v/v) at 275 °C for 30 min. This difference could be due to the higher ash content (4.97%) of Eupatorium adenophorum Spreng because higher amount of mineral matter may catalyze the decarbonylation reaction [37]. The small fraction of H_2 at higher temperatures could be due to water–gas shift and steam-reforming reactions [43]. From the energy point of view, the permanent gases were characterized by a low heating value between 2 and 3.5 MJ/Nm^3; however, after appropriate purification and concentration, the non-condensable gases could be useful burned in order to partially satisfy the energy requirements of the torrefaction plant.

Table 5
Product yields and HHV of non-condensable gases at different torrefaction temperatures.

Product	210 °C	235 °C	260 °C
H_2 (wt%)	0	0.001	0.001
CO (wt%)	0.241	0.388	1.631
CO_2 (wt%)	2.599	2.614	8.799
C_3H_8 (wt%)	0.010	0.015	0.064
C_5H_{12} (wt%)	0	0.001	0.012
C_6H_{14} (wt%)	0	0	0.004
Higher Heating Value (MJ/Nm^3)	1.95	2.92	3.55

3.4. Characterization of liquid products

Water was the major condensable product of SCG torrefaction process, with a percentage of 91.9%, 80.9%, and 73.7% at the temperature of 210 °C, 235 °C, and 260 °C, respectively. Water was mainly released from the evaporation of freely bound water and the chemical dehydration and condensation reactions between organic molecules [13]. In particular, the water content of liquid products decreased when the torrefaction temperature increased because the tar production raised due to the decomposition and devolatilization of hemicellulose. Tar was formed by a complex mixture of acids, alcohols, ketones, aldehydes, phenols, and furans. Fig. 4 shows that acids were the second most abundant product in the liquid fraction, mostly due to the production of acetic acid (about 77% of the acids at all temperatures) from the degradation of acetoxy- and methoxy-groups contained in the hemicellulose, mainly in xylan [11].

In addition to the acids, the production of furans, ketones and aldehydes was also pronounced starting from the temperature of 235 °C, due to the cleavage of pyranose rings in holocellulose [31]. At 260 °C the two main chemical species in the furanic, ketonic and aldehydic compounds were hydroxyacetone (81.8%), and furfural (10.5%). The yield of hydroxyacetone (about 1.6 wt%) was higher than that obtained for other biomass such as pine (0.6 wt%), ash-wood (0.6 wt%) and wheat straw (1.3 wt%) during the torrefaction process at 280 °C for 45 min [14]. This result could be explained by the fact that hydroxyacetone is formed from the breakdown of the cellulose fibrils that are

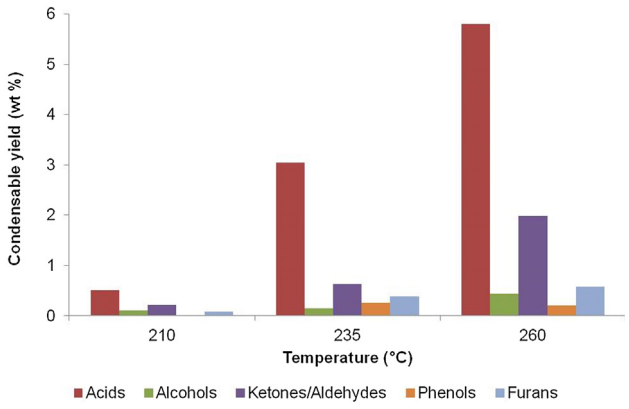

Fig. 4. Product yields of tar at different torrefaction temperatures.

Table 6
Elemental analysis and HHV of tar obtained at different torrefaction temperatures.

Temperature (°C)	C (wt % db)	H (wt % db)	N (wt % db)	O (wt % db)	Higher Heating Value (MJ/kg db)
210	48.5 ± 0.9	6.6 ± 0.5	2.8 ± 0.1	42.2 ± 1.1	18.8 ± 0.9
235	50.9 ± 1.3	6.0 ± 0.3	2.2 ± 0.1	40.9 ± 1.0	19.3 ± 0.6
260	57.7 ± 0.7	7.0 ± 0.4	2.1 ± 0.2	33.3 ± 0.6	23.4 ± 0.8

Table 7
Industrial uses of the main condensable products.

Compounds	Yield (wt%)			Uses	Refs.
	210 °C	235 °C	260 °C		
Lactic acid	0.03	0.35	0.70	Used as a preservative and pH adjusting agent in the food and beverage industry and for production of lactate ester	[46]
Formic acid	0.08	0.26	0.31	Used for animal feed protection, textiles and leather processing, flue gas desulfurization and to manufacture pharmaceuticals	[47]
Acetic acid	0.40	2.28	4.11	Used for production of foam rubber, wood gluing, emulsifiers, cement coatings and desalination membranes	[46]
Levulinic acid	0.00	0.12	0.57	Used to produce pharmaceuticals, synthetic fibers and plastics and as an intermediate for higher value-added chemical compounds, such as methyl vinyl ketone and olefins	[48,49]
Methanol	0.11	0.14	0.41	Used for production of formaldehyde, methyl-tert-butyl ether (MTBE), acetic acid and dimethyl ether. It is also used as a fuel in addition togasoline and for the denitrification process in the wastewater treatment plants	[50]
Furfural	0.04	0.36	0.49	Used for production of adhesives, as flavor compound and to replace oil-based chemicals	[46]
Acetone	0.00	0.33	0.68	Used for production of acrylic plastics, signs, lighting fixtures, displays and as a solvent in paints, cleaning fluids, and adhesives	[46]
Hydroxyacetone	0.26	0.21	1.56	Used in the food sector (as flavouring compound), in the cosmetic industry (as a skin tanning agent) and in the textile industry (as a reduced dye) and for the production of chemical compounds, such as propylene glycol and acrolein	[51]

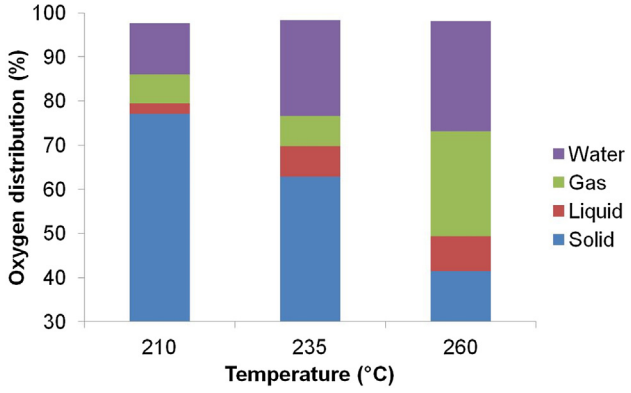

Fig. 5. Oxygen distribution in torrefaction products.

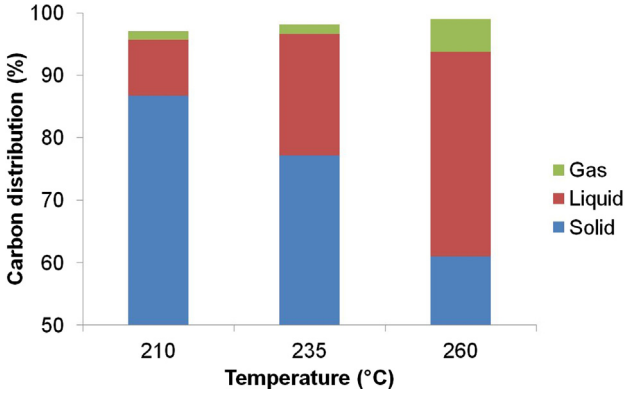

Fig. 6. Carbon distribution in torrefaction products.

protected by lignin. SCG contains lower proportions of lignin than other lignocellulosic biomass, thus cellulose in SCG would be less protected from thermal degradation. Among the alcohols, the main one was methanol with a yield that increased rapidly over the temperature of 235 °C. At 260 °C, about 0.4 wt% yield of methanol was obtained, mostly due to decomposition of the methoxyl groups present both in the

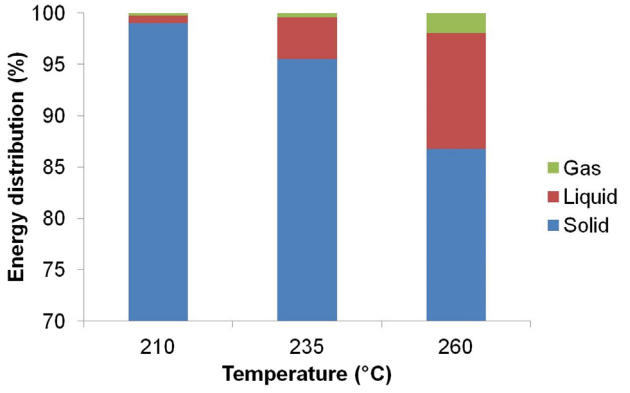

Fig. 7. Energy distribution in torrefaction products.

Table 8
Energy yield (EY) and energy density enhancement (EDE) obtained at different torrefaction temperatures.

Temperature (°C)	EY	EDE
210	90.2	5.1
235	79.5	7.5
260	64.4	15.4

4-O-methylglucuronic acid unit linked to the xylan chain and in the lignin structure [44].

Tar composition was highly influenced by the torrefaction temperature and this result was confirmed by the elemental analysis reported in Table 6. It can be noted that carbon content of tar increased from 48.5% to 57.7% as the torrefaction temperature increased from 210 °C to 260 °C, due to the higher content of organic compounds. At the same time, the oxygen content tends to decline together with the atomic O/C ratio, whose value decreases from 0.65 to 0.43. Based on the elemental composition, HHV of tar was also calculated; obviously, the lowest value of HHV (18.8 MJ/kg db) was obtained at the lowest torrefaction temperature, corresponding to the highest value of the oxygen content. The highest value (23.4 MJ/kg db) was of the same

order of magnitude as that of pyrolysis bio-oil (23.9–26.8 MJ/kg) [45]. However, its high moisture content requires a dehydration process before use as a fuel or for the production of chemicals.

The condensable products from torrefaction gas can be considered as by-products of the process because they may be applied in several industrial fields either as precursors for other products or as solvents. Table 7 shows a summary of the industrial applications of the main compounds obtained in the condensable fraction.

3.5. Oxygen, carbon and energy distribution

Fig. 5 shows the oxygen distribution among the torrefied SCG, tar, water, and gas at different torrefaction temperatures. It can be noted that, as the temperature increased, the oxygen content in the torrefied SCG decreased, migrating to the liquid and gaseous products in the form of oxygen-containing organic compounds, water, CO, and CO2. Up to the temperature of 235 °C, the deoxygenation reactions mainly lead to the formation of water while, when the torrefaction temperature reached 260 °C, also gaseous products became a significant contributor of oxygen transfer and only 59% of oxygen was still retained in the solid product. On the other hand, within the torrefaction temperature range of 210–260 °C, only 2.4–7.8% of oxygen was transformed into the tar, demonstrating that the main deoxygenation pathway was the release of non-condensable products and water.

Along with the deoxygenation process, the torrefaction treatment causes also the decarbonization of the solid product. As shown in Fig. 6, carbon mainly remained in the solid fraction but its proportion decreased from 86.8% to 61.0% within the torrefaction temperature range. In particular, a very small fraction of carbon was transferred to the gaseous products, showing that the most significant decarbonization pathway was the release of tar. Since deoxygenation leads to increase the HHV of biomass and decarbonization causes a loss of energy from the solid product, both processes have a considerable effect on the energy distribution of SCG. Fig. 7 shows that, as the torrefaction temperature increased, the energy fraction of the solid product decreased, even if most of the energy of SCG was retained in the torrefied SCG with values from 99.0% to 86.8% within the torrefaction temperature range. Furthermore, it can be observed that non-condensable products were characterized by the lowest value of the energy yield (0.3–2.0%) at all temperatures, due to the low yield and the low calorific value of gas.

Energy yield and energy density enhancement are the most important parameters to establish the effectiveness of the torrefaction treatment [36]. Table 8 shows that the highest value of EY was obtained at the temperature of 210 °C but the simultaneous increase in HHV was quite low. In particular, the EDE increased sharply with the torrefaction temperature for values higher than 235 °C. Therefore, the temperature of 260 °C would seem the best suitable torrefaction condition to upgrade SCG, giving a significant enhancement of HHV and retaining about two-thirds of the energy content in the raw material.

4. Conclusions

The aim of this work was to contribute to better understand the chemical evolution of the solid, condensable and non-condensable phases produced during SCG torrefaction in a continuous horizontal rotary reactor having a production capacity of 500 kg/h. Three operating temperatures (210 °C, 235 °C, 260 °C) for 90 min were selected as the torrefaction conditions. Results showed that temperature had a significant influence on the process parameters, such as mass and energy yields, mostly when the value was above 235 °C. With increasing torrefaction temperature, the energy density enhancement increased, mainly due to the decomposition of hemicellulose and cellulose in the raw material. At 260 °C the hemicellulose content in the torrefied SCG was reduced to 3.3%, demonstrating a significant effectiveness of the deoxygenation process. Most of the oxygen removed was transferred to the water and non-condensable fractions. On the other hand, the decarbonisation process caused a significant migration of carbon mostly into the liquid products (about 33% at 260 °C). Tar fraction was composed mainly of acetic acid and hydroxyacetone and about 11% of the feedstock energy was retained in it at 260 °C. However, high moisture content of condensable fraction (73.7% at 260 °C) affects the employment as a fuel but suggesting its use as a chemicals' source. This study demonstrated at a semi-industrial scale that torrefaction is an interesting option to pretreat SCG in order to produce a fuel with improved energy density.

Declaration of Competing Interest

The authors declare that they have no known competing financial interests or personal relationships that could have appeared to influence the work reported in this paper.

Acknowledgements

This work was partially funded by the European Union's Horizon 2020 Research and Innovation Programme under grant agreement number 731101 (BRISK 2 project).

References

[1] EUROSTAT. Energy Balance Sheets – 2016 Data, 2018 edition. Publications Office of the European Union, Luxembourg; 2018.
[2] Lu D, Yoshikawa K, Ismail TM, Abd El-Salam M. Assessment of the carbonized woody briquette gasification in an updraft fixed bed gasifier using the Euler-Euler model. Appl Energy 2018;220:70–86.
[3] Plaza MG, González AS, Pevida C, Pis JJ, Rubiera F. Valorisation of spent coffee grounds as CO_2 adsorbents for postcombustion capture applications. Appl Energy 2012;99:272–9.
[4] Cervera-Mata A, Pastoriza S, Rufián-Henares JA, Párraga J, Martin-García JM, Delgado G. Impact of spent coffee grounds as organic amendment on soil fertility and lettuce growth in two Mediterranean agricultural soils. Arch Agron Soil Sci 2018;64(6):790–804.
[5] Mata TM, Martins AA, Caetano NS. Bio-refinery approach for spent coffee grounds valorization. Bioresour Technol 2018;247:1077–84.
[6] Chen W-H, Lin B-J, Colin B, Chang J-S, Petrissans A, Bi X, et al. Hygroscopic transformation of woody biomass torrefaction for carbon storage. Appl Energy 2018;231:768–76.
[7] Larsson SH, Rudolfsson M, Nordwaeger M, Olofsson I, Samuelsson R. Effects of moisture content, torrefaction temperature, and die temperature in pilot scale pelletizing of torrefied Norway spruce. Appl Energy 2013;102:827–32.
[8] Bridgeman TG, Jones JM, Shield I, Williams PT. Torrefaction of reed canary grass, wheat straw and willow to enhance solid fuel qualities and combustion properties. Fuel 2008;87(6):844–56.
[9] Bilgic E, Yaman S, Haykiri-Acma H, Kucukbayrak S. Limits of variations on the structure and the fuel characteristics of sunflower seed shell through torrefaction. Fuel Process Technol 2016;144(Supplement C):197–202.
[10] Macedo LAd, Commandré J-M, Rousset P, Valette J, Pétrissans M. Influence of potassium carbonate addition on the condensable species released during wood torrefaction. Fuel Process Technol 2018;169:248–57.
[11] Nhuchhen DR, Basu P, Acharya B. A comprehensive review on biomass torrefaction. Int J Renew Energy Biofuels 2014:1–56.
[12] Detcheberry M, Destrac P, Massebeuf S, Baudouin O, Gerbaud V, Condoret JS, et al. Thermodynamic modeling of the condensable fraction of a gaseous effluent from lignocellulosic biomass torrefaction. Fluid Phase Equilib 2016;409:242–55.
[13] Doddapaneni TRKC, Praveenkumar R, Tolvanen H, Rintala J, Konttinen J. Techno-economic evaluation of integrating torrefaction with anaerobic digestion. Appl Energy 2018;213:272–84.
[14] Lê Thành K, Commandré JM, Valette J, Volle G, Meyer M. Detailed identification and quantification of the condensable species released during torrefaction of lignocellulosic biomasses. Fuel Process Technol 2015;139:17–9.
[15] Christoforou E, Fokaides PA. Solid Biomass Pretreatment Processes. In: Advances in Solid Biofuels. Green Energy and Technology; 2019.
[16] Chen WH, Liu SH, Juang TT, Tsai CM, Zhuang YQ. Characterization of solid and liquid products from bamboo torrefaction. Appl Energy 2015;160:829–35.
[17] Zhang C, Ho SH, Chen WH, Xie Y, Liu Z, Chang JS. Torrefaction performance and energy usage of biomass wastes and their correlations with torrefaction severity index. Appl Energy 2018;220:598–604.
[18] IEA Bioenergy/Task 33. Gas analysis in gasification of biomass and waste - guideline report - Document 1; 2018.
[19] Nhuchhen DR, Basu P, Acharya B. Torrefaction of poplar in a continous two-stage, indirectly heated rotary torrefier. Energy Fuels 2016;30:1027–38.
[20] Strandberg M, Olofsson I, Pommer L, Wiklund-Lindström S, Åberg K, Nordin A. Effects of temperature and residence time on continuous torrefaction of spruce wood. Fuel Proc Technol 2015;134:387–98.

[21] Campbell WA, Woytiuk K, Gerspacher R, Coller A, Evitts RW. Char quality response surfaces from torrefaction of coppiced willow in a horizontal moving bed pilot plant. Can J Chem Eng 2019;97:84–92.
[22] Severy MA, Chamberlin CE, Eggink AJ, Jacobson AE. Demonstration of a pilot-scale plant for biomass torrefaction and briquetting. Appl Eng Agric 2018;34:85–98.
[23] Li H, Liu X, Legros R, Bi XT, Lim CJ, Sokhansanj S. Torrefaction of sawdust in a fluidized bed reactor. Bioresour Technol 2012;103:453–8.
[24] Brachi P, Miccio F, Miccio M, Ruoppolo G. Torrefaction of tomato peel residues in a fluidized bed of inert particles and a fixed-bed reactor. Energy Fuels 2016;30:4858–68.
[25] Chen WH, Peng J, Bi XT. A state-of-the-art review of biomass torrefaction, densification and applications. Renew Sust Energ Rev 2015;44:847–66.
[26] Granados DA, Velásquez HI, Chejne F. Energetic and exergetic evaluation of residual biomass in a torrefaction process. Energy 2014;74:181–9.
[27] Buratti C, Barbanera M, Lascaro E, Cotana F. Optimization of torrefaction conditions of coffee industry residues using desirability function approach. Waste Manage 2018;73:523–34.
[28] Agar D, Gil J, Sanchez D, Echeverria I, Wihersaari M. Torrefied versus conventional pellet production – a comparative study on energy and emission balance based on pilot-plant data and EU sustainability criteria. Appl Energy 2015;138:621–30.
[29] Cotana F, Buratti C, Barbanera M, Lascaro E. Optimization of the steam explosion and enzymatic hydrolysis for sugars production from oak woods. Bioresour Technol 2015;198:470–7.
[30] Koppejan J, Sokhansanj S, Melin S, Madrali S. Status overview of torrefaction technologies. International Energy Agency, IEA Bioenergy Task 32 report; 2012.
[31] Han Z, Zeng X, Yao C, Xu G. Oxygen migration in torrefaction of Eupatorium adenophorum Spreng. and its improvement on fuel properties. Energy Fuels 2015;29(11):7275–83.
[32] Nhuchhen DR, Basu P, Acharya B. Torrefaction of poplar in a continous two-stage, indirectly heated rotary torrefier. Energy Fuels 2016;30:1027–38.
[33] Sabil KM, Aziz MA, Lal B, Uemura Y. Synthetic indicator on the severity of torrefaction of oil palm biomass residues through mass loss measurement. Appl Energy 2013;111:821–6.
[34] Chen D, Gao A, Ma Z, Fei D, Chang Y, Shen. In-depth study of rice husk torrefaction: characterization of solid, liquid and gaseous products, oxygen migration and energy yield. Bioresour Technol 2018;253:148–53.
[35] Uemura Y, Omar WN, Tsutsui T, Yusup SB. Torrefaction of oil palm wastes. Fuel 2011;90:2585–91.
[36] Nhuchhen DR, Afzal MT, Parvez AM. Effect of torrefaction on the fuel characteristics of timothy hay. Biofuels 2018. https://doi.org/10.1080/17597269.2018.1479135.
[37] Prins MJ, Ptasinski KJ, Janssen FJJG. Torrefaction of wood: Part 2. Analysis of products. J Anal Appl Pyrol 2006;77(1):35–40.
[38] van der Stelt MJC, Gerhauser H, Kiel JHA, Ptasinski KJ. Biomass upgrading by torrefaction for the production of biofuels: a review. Biomass Bioenergy 2011;35(9):3748–62.
[39] Chen DY, Zhou JB, Zhang QS, Zhu XF, Lu Q. Upgrading of rice husk by torrefaction and its influence on the fuel properties. Bioresources 2014;9(4):5893–905.
[40] Iroba KL, Baik OD, Tabil LG. Torrefaction of biomass from municipal solid waste fractions II: Grindability characteristics, higher heating value, pelletability and moisture adsorption. Biomass Bioenergy 2017;106:8–20.
[41] Brito JO, Silva FG, Leão MM, Almeida G. Chemical composition changes in eucalyptus and pinus woods submitted to heat treatment. Bioresour Technol 2008;99:8545–8.
[42] Tumuluru SJ, Sokhansanj S, Wright TC, Boardman DR, Hess RJ, Review on biomass torrefaction process and product properties and design of moving bed torrefaction system model development, ASABE Annual International Meeting. Louisville, Kentucky USA; 2011.
[43] Wei L, Gao Y, Qu W, Zhao X, Cheng S. Torrefaction of raw and blended corn stover, switchgrass, and prairie grass. Trans ASABE 2016;59:717–26.
[44] Chang S, Zhao Z, Zheng A, He F, Huang Z, Li H. Characterization of products from torrefaction of sprucewood and bagasse in an auger reactor. Energy Fuels 2012;26(11):7009–17.
[45] Brassard P, Godbout S, Raghavan V. Pyrolysis in auger reactors for biochar and bio-oil production: a review. Biosyst Eng 2017;161:80–92.
[46] Rosales-Calderon O, Arantes V. A review on commercial-scale high-value products that can be produced alongside cellulosic ethanol. Biotechnol Biofuels 2019;12:240.
[47] Rauch S, Piepenbreier F, Voss D, Albert J, Hartmann M. LCA in Process Development: Case Study of the OxFA-Process. In: Schebek L, Herrmann C, Cerdas F, editors. Progress in Life Cycle Assessment. Sustainable Production: Life Cycle Engineering and Management. Springer; 2019. p. 105–13.
[48] Sandhu SK, Mathur A, Gupta R, Puri SK, Adsul M. Cellulosic Biomass-Hydrolyzing Enzymes. In: Singhania R, Agarwal R, Kumar R, Sukumaran R, editors. Waste to Wealth. Energy, Environment, and Sustainability. Springer; 2018, pp. 441–456.
[49] Abaide ER, Ugalde G, Luccio MD, Moreira RFPM, Tres MV, Zabot GL, Mazutti MA. Obtaining fermentable sugars and bioproducts from rice husks by subcritical water hydrolysis in a semi-continuous mode. Bioresour Technol 2019;272:510–20.
[50] Biernacki P, Tobias R, Paul W, Werner P, Steinigeweg S. Environmental impact of the excess electricity conversion into methanol. J Clean Prod 2018;191:87–98.
[51] Bharti A, Verma R, Prerna N, Sarvesh A, Malviya T, Banerjee T, et al. Liquid-liquid equilibria and COSMO-SAC modeling of organic solvent/ionic liquid - hydroxyacetone - water mixtures. Fluid Phase Equilibr 2018;462:73–84.